Working speed optimization of the fully automated vegetable seedling transplanter

Bhola Paudel,[1,4] Jayanta Kumar Basak,[2] Seong Woo Jeon,[3] Gun Ho Lee,[3] Nibas Chandra Deb,[4] Sijan Karki,[4] Hyeon Tae Kim[4]

[1]Future Regions Research Centre, Ararat Jobs and Technology Precinct, Federation University, Ballarat, Australia; [2]Institute of Smart Farm, Gyeongsang National University, Jinju; Korea; [3]Department of Smart Farm, Graduate School, Gyeongsang National University, Jinju, Korea; [4]Department of Biosystems Engineering, Institute of Smart Farm, Gyeongsang National University, Jinju, Korea

Abstract

The purpose of this study was to determine the optimal operating speeds for a low-speed automated vegetable transplanter that utilized a modified linkage cum hopper-type planting unit. A biodegradable seedling plug-tray feeding mechanism is employed by the transplanter. Using kinematic simulation software, the planter unit's movement was simulated under various operating conditions. The resulting trajectories were compared based on variables like plant spacing, soil intrusion area, soil intrusion perimeter, and horizontal hopper displacement in the soil. It was discovered that the best results occurred at 200, 250, and 300 mm/s and 40, 50, and 60 rpm combinations. Following testing in a soil bin facility, it was discovered that the ideal operating speeds performed well when transplanting pepper seedlings, with measured plant spacing that was nearly identical to the theoretical spacing. While the planting angle in various speed combinations was found to be significantly different, but still within acceptable bounds, the planting depth in each case did not differ statistically. The optimal speed combinations that were chosen resulted in minimal damage to the mulch film. The best speeds for the transplanter were found through this investigation, and these speeds can be used as a foundation for refining the other mechanisms in the transplanter.

Introduction

Farming vegetables in Korea accounted for about 23% of the total farm population in 2021, which increased by 7.5% compared to 2020 (Statistics Korea, 2021). Vegetable products are the most consumed all around the world because of their important role as a nutrition source for humans (Kalmpourtzidou *et al*., 2020). There are two ways to grow vegetables in fields: first, by directly sowing seeds in the field for crops such as beans and okra, and second, by preparing seedlings in nursery beds and transplanting them to the field for crops such as tomatoes and peppers (Kumar and Raheman, 2011). The transplantation of seedlings into the field can be done manually using human resources or with seedling transplanting machinery. Manually transplanting seedlings into the field is a labor-intensive and time-consuming task, taking around 40% of the overall operation time, or about 184 person-hours per hectare (Iqbal *et al*., 2021b; Kumar and Raheman, 2008; Park *et al*., 2005b). This can be a problem during peak agricultural season when there is a shortage of farm labor. To reduce the dependency on human labor and meet the growing demand for vegetable crops, farm operations need to be mechanized, starting with the labor-intensive task of transplantation (Park *et al*., 2005a).

There are various mechanisms equipped within transplanting

Correspondence: Hyeon Tae Kim, Department of Biosystems Engineering, Institute of Smart Farm, Gyeongsang National University, Jinju, 52828, Korea.
Tel.: +82.557721896.
E-mail: bioani@gnu.ac.kr

Key words: optimization; performance; planter mechanism; solidworks; vegetable transplanter.

Acknowledgments: the authors would like to thank the Korea Institute of Planning and Evaluation for Technology in Food, Agriculture and Forestry (IPET) through the Agriculture, Food and Rural Affairs Convergence Technologies Program for Educating Creative Global Leader Program, funded by the Ministry of Agriculture, Food and Rural Affairs (716001-7) for financial support to conduct the research.

Contributions: BP, responsible for all calculations, figures, writing, and editing large portions of the text; JKB, supervision of the study and review; SWJ, GHL, NCD, SK, help during the experimental setup and data collection period; HTK, review and editing, guide of the experiment. All the authors approved the final version to be published.

Conflict of interest: the authors declare no potential conflict of interest.

Funding: this research has been financially supported by the Korea Institute of Planning and Evaluation for Technology in Food, Agriculture and Forestry (IPET) through the Agriculture, Food and Rural Affairs Convergence Technologies Program for Educating Creative Global Leader Program, funded by the Ministry of Agriculture, Food and Rural Affairs (MAFRA) (716001-7).

Availability of data and material: the datasets generated and/or analyzed during the current study are available from the corresponding author upon reasonable request.

Received: 26 December 2022.
Accepted: 10 May 2023.

Journal of Agricultural Engineering 2024; LV:1569
doi:10.4081/jae.2024.1569

machines, including seedling selection and movement, seedling metering, and seedling planting mechanisms, which are important to consider when designing an efficient transplanter (Islam *et al*., 2022; Wen *et al*., 2021). When designing these mechanisms, special attention should be given to the seedling planting mechanism, as the ultimate goal of a vegetable transplanter is to transplant seedlings into the soil at the correct position without damaging them (Iqbal *et al*., 2021a). The spacing, depth, and alignment of transplanted seedlings, as well as the planting rate, misplanting rate, and working efficiency, can be controlled and determined through the operating motion of the planter (Shim *et al*., 2016). During transplanting, the planter hopper should follow an ideal trajectory that allows it to insert into the soil with a minimum push force, leave the seedling at the proper depth and alignment, and withdraw from the soil without affecting the transplanted seedling (Jin *et al*., 2020). To determine the ideal trajectory for the planter and verify the design parameters, kinematic analysis of the mechanism must be conducted (Islam *et al*., 2020; Reza *et al*., 2021). Previous research has included the development of mathematical models for seedling transplanting mechanisms using matrix laboratory software (MATLAB) (Liu *et al*., 2009), the design of a two-row walk-behind transplanter for seedlings prepared in paper pots (Kumar & Raheman, 2011), the study of the operating characteristics and testing of the transplanting performance of semi-automated commercial transplanters (Park *et al*., 2018), the optimization of the link length of semi-automated transplanters to reduce the weight of the planter unit while maintaining the same working trajectory using genetic algorithms (Hwang *et al*., 2020), and the analysis of the effect of different working speeds on the performance and power consumption of dibbling planters (Iqbal *et al*., 2021).

The operations of other mechanisms within the transplanter, such as seedling selection, movement, and metering mechanisms, depend on the forward speed at which the planter unit is working. In other words, all the mechanisms involved in the transplanter need to be properly synchronized. The desired planting interval, planting depth, and higher transplanting efficiency can only be achieved if all the working mechanisms are synchronized properly (Durga *et al*., 2020; Sri *et al*., 2022). Therefore, it is very important to determine the suitable working speed for the automated transplanter's planter unit so that the seedling supply rate can be synchronized (Iqbal *et al*., 2021b). Additionally, during high-speed transplantation, there is a risk of mechanically damaging the seedling during metering and transplanting, excessively damaging the plastic mulching film during dibbling action, and distorting the uprightness (high planting angle) of the seedling, which can affect plant growth and yield (Dou *et al*., 2021). As a result, the optimized speed for the planter unit needs to be determined and tested before it is fixed to the transplanter.

Gyeongsang National University's Smart Farm System laboratory aims to develop a linkage cum hopper-type automated vegetable transplanter that uses a biodegradable seedling plug-tray to prepare the seedlings. The biodegradable seedling plug trays will be fed directly into the transplanter, where the cutting mechanisms separate individual plug-cells with seedlings and pass them to the planter unit (hopper) for transplantation. To design an effective plug-tray-cutting mechanism, the forward speed of the transplanter, rotational speed of the planter unit, and working speed of the plug-tray-cutting mechanisms must be properly synchronized. To design an effective plug-tray-cutting mechanism, it is necessary to study the speed of the transplanter and its effect on the seedling transplanting properties. Therefore, this study aims to determine the suitable working speeds for the linkage cum hopper type planter unit of an automated vegetable transplanter and to determine the transplanting performance at these speeds, considering both agronomic and ergonomic requirements.

Materials and Methods

Description of the automated vegetable transplanter and planter unit

The vegetable transplanter considered for this study was the automated biodegradable seedling pot transplanter developed by the Smart Farm System Laboratory of Gyeongsang National University (Figure 1). According to the design of the transplanter, its key feature is the use of a biodegradable seedling pot where the cutting mechanism cuts and separates each plug-cell from the plug-tray and delivers the biodegradable plug-cells to the planting unit. For the automated vegetable transplanter, a linkage cum hopper-type planting unit was selected. The proposed transplanter is battery-powered, with 12-volt and 100-ampere batteries, and direct current motors control its movement. The transplanter consists of three major units: the control unit, the plug-tray-cutting unit, and the planter unit. The control unit consists of the controller parts that control the movement of the motors associated with different components of the transplanter. The plug-tray-cutting unit is where the plug-trays of 12×8 cells with seedlings are placed. When the hopper reaches the topmost position of its trajectory, each individual cell with a seedling is separated and dropped into the hopper of the planter unit. The function of the planter unit is to put the seedling into the soil at the desired depth and alignment with minimal damage to the soil and mulching film. The planter mechanism used for this study was a modified version of the linkage-type vegetable transplanter (KTP-30N, KM International, Seoul, South Korea). The modification was performed by Jo *et al*., (2018) to improve the transplanting performance by optimizing the link length, which mostly influenced the trajectory of the hopper endpoint.

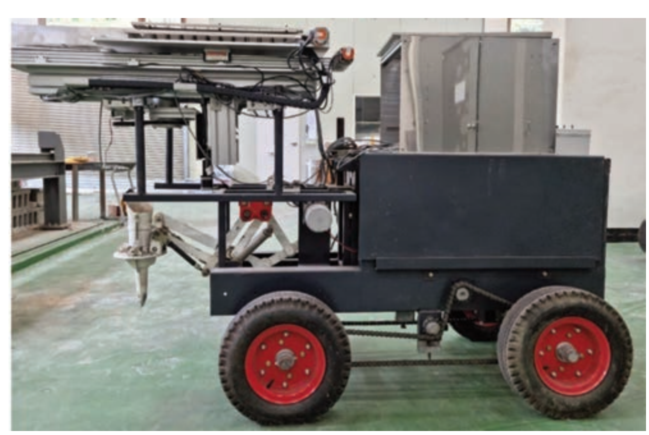

Figure 1. The developed automated vegetable transplanter that requires speed optimization. The transplanter is battery-powered with direct current motors to control its movements.

Theoretical analysis

Planter unit

The planter mechanism used for this study was the modified version of the linkage-type vegetable transplanter (KTP-30N, KM International, Seoul, South Korea). The link structure of the transplanting device is shown in Figure 2. The link structure of the transplanting device can be understood by dividing it into three parts: the first part, *i.e.*, link L_1, L_2, L_3,and L_4 (Joint BCDEF) is a four-bar link with link CD as crank, L_3 as a ternary link and L_1 as ground; the second part, *i.e.*, link L_1, L_6, L_7, and L_8 (joint ABGIH) is also a four-bar link with L_8 as a ternary link; and the third part, *i.e.*, link L_5, L_8, L_9, and L_{10} as a four bar link in which link L_{10} is a hopper part of the planter device. Equations 1-6 describe the position and angles of the various linkage parts (Jo *et al*., 2018).

$$S_1 = \sqrt{BC^2 + CD^2 - 2BC^2CD^2\cos\theta} \quad (1)$$

$$\gamma = \cos^{-1}\left(\frac{DE^2 + BE^2 - BD^2}{2\,DE\,BE}\right) \quad (2)$$

$$\omega = 180^0 - \cos^{-1}\left(\frac{DE^2 + BE^2 - BD^2}{2\,DE\,BE}\right) \quad (3)$$

$$S_2 = \sqrt{BE^2 + EF^2 - 2BE^2EF^2\cos\theta} \quad (4)$$

$$\alpha = \cos^{-1}\left(\frac{EF^2 + BF^2 - BE^2}{2\,EF\,BF}\right) \quad (5)$$

$$\beta = \cos^{-1}\left(\frac{FG^2 + BF^2 - BG^2}{2\,FG\,BF}\right) \quad (6)$$

Ideal transplanting conditions

In a fully automated vegetable transplanter, seedlings are automatically fed into the planting unit through the seedling supply mechanism (Tsuga, 2000). The planter unit then releases the seedlings into the soil at desired/specified points. The seedling supply and planting mechanisms must repeat this task consecutively for the planting operation to be carried out. The repeated motion of the planter unit can be studied through its working trajectory (Figure 3). To optimize the work of the planter unit for fast and

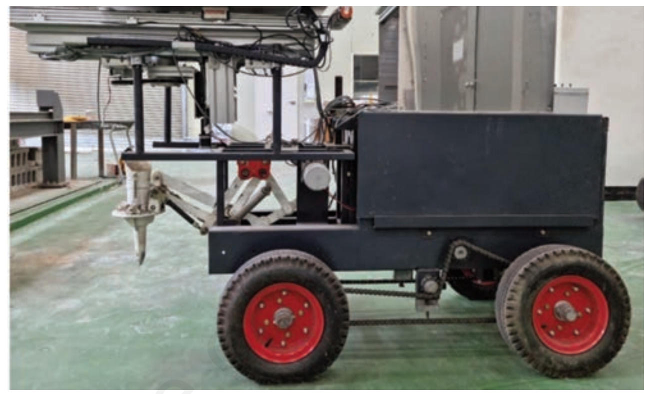

Figure 1. The developed automated vegetable transplanter that requires speed optimization. The transplanter is battery-powered with direct current motors to control its movements.

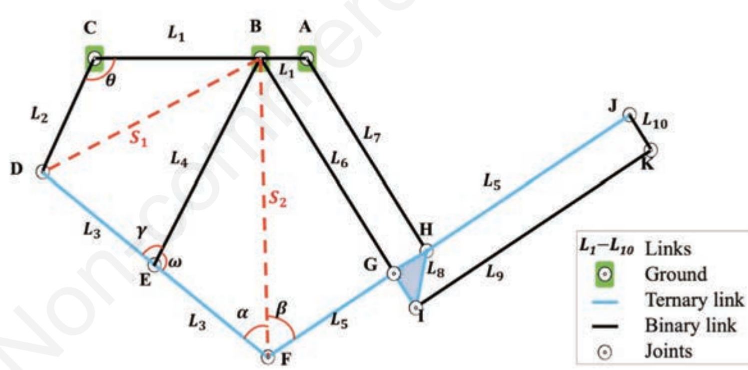

Figure 2. Link design of the transplanters' seedling planter unit showing different link types and joints.

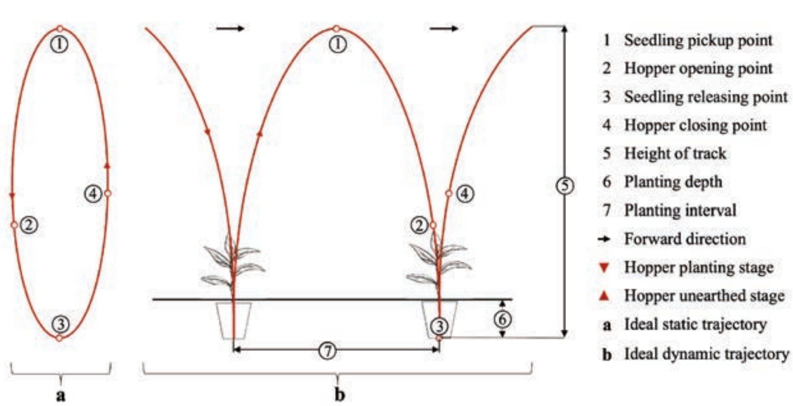

Figure 3. The ideal static and dynamic trajectory of the planter unit for effective transplanting.

accurate planting, the planter unit and the trajectory made by its hopper end must meet certain requirements. Firstly, the theoretical design of the planter unit should have no blind spots, which ensures smooth movement of the planter. Secondly, the hopper of the planter unit should maintain a vertical position when releasing the seedling and when coming out of the soil. The vertical position of the hopper ensures that the planted seedling remains upright in the soil and that there is no physical damage to the seedling. Lastly, the effectiveness of the transplanter increases when the hopper achieves zero speed while receiving the seedling at its topmost position and releasing it at the lowermost position. Zero speed at the topmost position ensures that there is no damage to the seedling while the seedling is transferred from the supply mechanisms to the hopper. Similarly, the uprightness of the seedling can be ensured when the hopper achieves zero speed at the lowermost position.

Experimental design and methodology

To determine the suitable working speeds for the selected planter unit, this study utilizes sequential exploratory design (SED). SED is a mixed-method research approach that involves collecting and analyzing quantitative data first, followed by collecting and analyzing qualitative data to provide a more comprehensive understanding of the research problem (Edmonds and Kennedy, 2017). This study employs computer simulations, *i.e.*, Linkage and Solidworks to gather quantitative data on determining the optimal operating speed for the planter unit based on factors such as plant spacing, soil intrusion area, soil intrusion perimeter, and horizontal displacement of the hopper in soil. It then uses a soil bin facility to collect qualitative data on planter performance and calculate additional factors, such as planting depth, planting angle, and area of mulch film damage. The detailed methodology followed is described subsequently.

Model design verification

To verify the new design with the existing prototype of the planter unit, the simulated and real trajectories were compared. The real planting trajectory of the hopper endpoint during the operation was derived using a high-speed camera setup (Chronos 1.4, Kron Technologies Inc, Canada) in both static and dynamic conditions. For the static trajectory, the transplanting machine was set at rest and in a fixed position by applying the brake, while the hopper

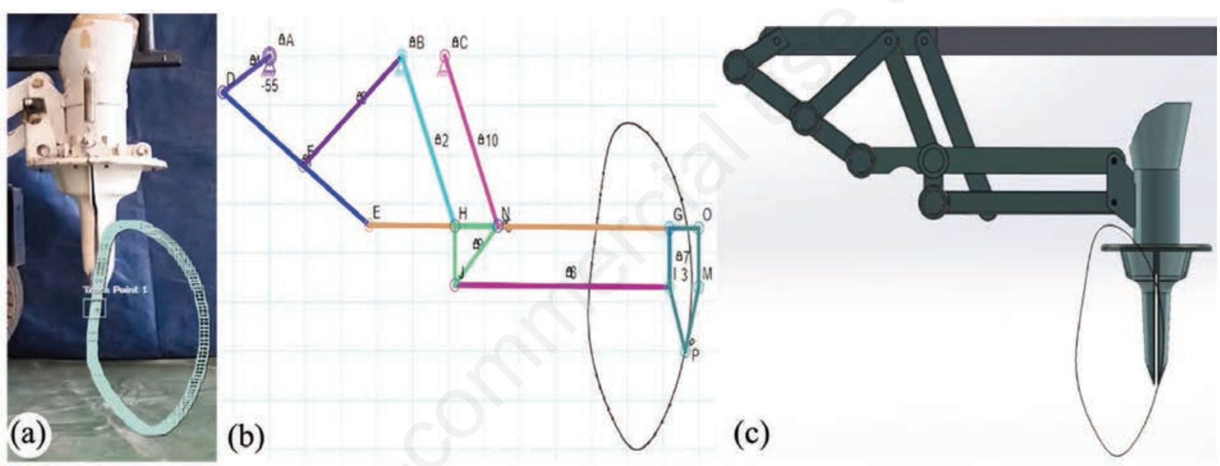

Figure 4. Extracting the static trajectory from the real planter using a high-speed camera (**a**) and from the designed planter unit parts using commercial simulation software: Linkage (**b**) and Solidworks (**c**).

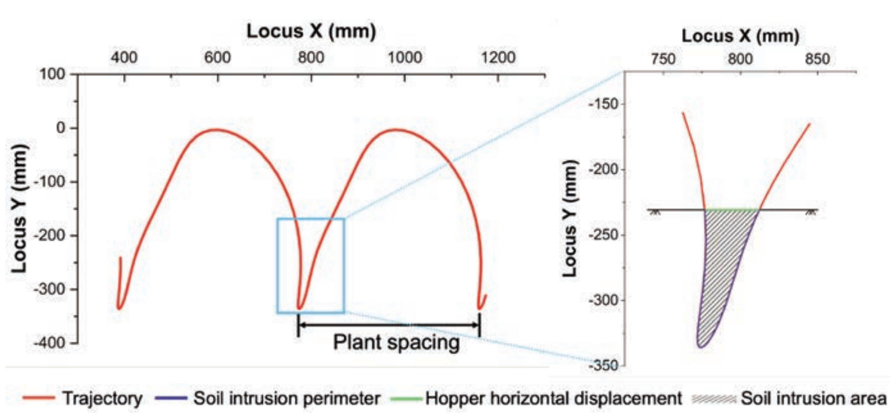

Figure 5. Sample of a simulated trajectory generated from Solidworks and methods to calculate the plant spacing, soil intrusion perimeter, horizontal hopper displacement in soil, and soil intrusion area from the simulated trajectory.

mechanism was operated at 30 revolutions per minute (rpm). For the dynamic trajectory determination, the transplanter machine was operated at a speed of 170 mm/s [similar to the condition mentioned by Jo *et al*. (2018)]. To detect and trace the position of the hopper end in each frame of the recorded video, a high-contrast object was placed at the lower point of the hopper (Figure 4a) such that it appears different from the color of the planter parts and surroundings and could be detected easily. Two points with a known distance were marked on the planters' frame as reference points to obtain the relative scale from the image and convert it to the absolute scale. The opening and closing of the hopper were restricted during the operation. During both processes, the video of the hopper movement was recorded using a high-speed camera at a resolution of 1280×1024 pixels and 1069 frames per second (fps). The recorded video was then downgraded to 120 fps and analyzed using Adobe After Effects 2021 (Adobe Inc., San Jose, California, USA). The motion tracking feature of the software was used to trace the position of the hopper end in each frame of the video. From the last frame of the video, two reference points were detected and marked to determine the scale of the trajectory. The traced points were extracted as a comma-separated value (CSV) file format and plotted on AutoCAD 2021 (Autodesk San Rafael, California, USA) for further comparison with other trajectories.

A Linkage Mechanism Designer and Simulator software (Linkage V.3.16.14, developed by David M. Rector, http://www.linkagesimulator.com) and a kinematic simulation software, *i.e.*, Solidworks 2022 (Dassault Systèmes, Waltham, Massachusetts, USA) were used to extract the simulated static and dynamic trajectories of the planting mechanism. In Linkage, a 2D model of the planter mechanism was prepared, and the links were studied to generate the static trajectory of the planter (Figure 4b). In Solidworks, a 3D model of the planter mechanism was created by measuring the actual dimensions of the components (Figure 4c). Since all the individual components of the planter were made of steel, the 3D model in Solidworks was designed using the properties of steel, *i.e.*, density: 7.85×10^3 kg/m^3; Poisson's ratio: 0.29; Young's modulus: 205 GPa; and Yield strength: 346.5 MPa. In the 3D model of the planter, the supporting frame was kept fixed while the planter crank could rotate at the desired rpm as per the rotation of the actual planter mechanism. Furthermore, a sliding panel was designed along with the frame to mimic the forward motion of the planter. During the static trajectory extraction, the forward speed was set to zero while the crank rotation was set to 30 rpm. For the dynamic trajectory, the forward speed was set to 170 mm/s and crank rotation of 30 rpm. During the simulation, the movement of the hopper end was traced to obtain the planting trajectory.

In order to verify the agreement between the planting trajectory obtained from the linkage and kinematic simulation software and the actual trajectory obtained from the high-speed camera measurement, an analysis of variance (ANOVA) test was performed. During the test, the planting trajectory obtained from the kinetic simulation software and linkage was set as the independent variable, while the planting trajectory obtained from the high-speed camera was set as the dependent variable. To derive the probability of significance, the X-coordinate value was targeted for the same Y-coordinate of both dependent and independent variables, according to the procedure of Hwang *et al*., (2020). For this, the linear interpolation method (Equation 7) was used to calculate the value for the X-coordinate for the same Y-coordinate value of both dependent and independent variables.

$$x = x_1 + \left(\frac{y - y_1}{y_2 - y_1}\right)\times(x_2 - x_1) \tag{7}$$

where, x_1 and y_1 are the preceding coordinates, x_1 and y_2 are the succeeding coordinates, y is the point at which the interpolation is performed, and x is the interpolated value.

Determination of optimum working and rotational speed

To determine the optimum speed for the transplanter, the planter unit was simulated for various running speeds. Several literatures on walking-type transplanters have suggested a running speed between 150-390 mm/s for ergonomics for the operator to walk behind the machine (Du *et al*., 2018; Kumar and Raheman, 2011; Park *et al*., 2005b). Therefore, in this study, the planter unit of the linkage-type was simulated within a forward speed range of 150 mm/s to 350 mm/s with an interval of 15 mm/s and different rotational speeds ranging from 30 rpm to 80 rpm with a difference of 5 rpm. From the trajectories generated from each working and rotational speed combination, the theoretical plant spacing, soil intrusion area, soil intrusion perimeter, and hopper horizontal displacement inside soil were calculated (Figure 5), plotting the trajectories in AutoCAD 2021.

However, it was very difficult to exactly meet the requirement for the ideal trajectory. Therefore, this study considered the minimum soil intrusion area, minimum soil intrusion perimeter, and minimum hopper horizontal displacement inside the soil as important considerations for selecting the optimized trajectory (Figure 5). The minimum soil intrusion area, intrusion perimeter, and horizontal displacement ensured that the hopper had the vertical altitude with the minimum X component of the linear velocity (v_X) towards the forward direction when the hopper reached the lower position inside the soil to release the seedling, and remained on vertical altitude after releasing until it came out of the soil. This also ensured no or minimal damage to the seedling with proper placement and alignment, as well as less damage to the plastic mulching film. Three working speeds and three rpm configurations were selected, resulting in the best trajectory condition to test in the soil test bin condition.

Testing of the planter mechanism

Seedlings of *Capsicum annuum* Linnaeus, a variety of pepper widely used in South Korea, were used to test the transplanting capabilities of the planter mechanism. The seedlings were germinated in paper-based biodegradable seedling pots in a controlled environment inside a plant factory (temperature 25°C and photoperiod 18 hours with LED lighting in the wavelength range of 440 nm to 680 nm) (Paudel *et al*., 2022) for 14 days and then transferred to a greenhouse for further growth and development. In the greenhouse, the seedlings were irrigated twice a day using an overhead sprinkler system, with each watering lasting five minutes. After 42 days, the seedlings were hardened for three days to enhance the strength of the plug trays.

The testing was performed in the soil test bin facility located at Gyeongsang National University. For this test, the planter mechanism was attached to the carriage. The carriage (Figure 6) consisted of two different motor assemblies with an independent power source, where the speed of each motor assembly can be controlled through the control panel. The first motor assembly consisted of dual motors located on each side of the carriage, responsible for the forward and backward speed of the carriage, while the second motor assembly consisted of a single motor located at the top of the carriage, connected using a V-belt and pulley to the crank, for varying the speed (rpm) of the planter mechanism.

Before the experiment, the test bin was filled with freshly extracted garden soil to a depth of 250 mm. The soil was leveled manually, and watering was done on alternate days to distribute the moisture evenly and to maintain the hardness of the soil within permissible limits, as suggested by previous research (Jo *et al.*, 2018), as the hardness and moisture content of the soil have an inverse relationship (r=-0.90). On the day of testing, soil samples were collected to measure the soil texture, electrical conductivity (EC), pH, moisture, and density with five replications. Pepper seedlings were manually fed into the hopper during its topmost position. The forward speed was maintained based on the time required to cover a known distance, while the crank rpm was adjusted using a digital tachometer (Model: Benetech GM8905, Shenzhen Wintact Electronics Co. Ltd, Shenzhen, China). For each speed and rpm combination, three replications were performed. The plant-to-plant distance (plant spacing), planting angle, planting depth, and mulching film damage were measured during each trial.

Data analysis

Data collected during the field test were recorded using Excel (Microsoft 365), and the collected data were analyzed using Statistical Package for the Social Sciences v.26 developed by IBM Corporation, Armonk, New York, USA. Mean values obtained during the test were compared using ANOVA, and statistically significant differences between means were identified using Tukey's honestly significant difference (HSD) *post hoc* test at a significance level of $p \leq 0.05$.

Results and Discussion

Verification with the planting trajectory

The static trajectory of the planter unit plays an important role in determining the opening and closing of the hopper unit. Point Ymax is the uppermost point of the hopper, where it receives the seedling from the metering and supply unit, and point Ymin is the lowest point, where the hopper enters into the soil and starts to release the seedling as it comes out. For the clockwise trajectory, the hopper should open after it has crossed the Xmax point and before it reaches Ymin, just as it enters the soil. The Xmin marks the point where the hopper closes to receive the seedling at Ymax (Jin *et al.*, 2020).

As per the linkage-derived static trajectory result, the maximum and minimum X coordinate values were 566.9 mm and 421.5 mm, respectively. The maximum and minimum Y coordinate values (Ymax, Ymin) were -3.2 mm and -336.2 mm, respectively. These results were very close to the static trajectory obtained from the Solidworks simulation, where the maximum and minimum X coordinate values (Xmax, Xmin) were 567.0 mm and 421.6 mm, respectively, and the maximum and minimum Y coordinates were -3.1 mm and -336.1 mm, respectively. Thus, the static trajectory's maximum height (Ymax - Ymin) was 333.0 mm, and the maximum width (Xmax - Xmin) was 145.4 mm. For the dynamic trajectory determined by Solidworks, the maximum height was 330.0 mm, equal to the maximum height of the static trajectory, and during three crank rotations, the planter had a horizontal displacement of 1020 mm (Xmin: 564.7 mm and Xmax: 1584.7 mm). For the real trajectory obtained from video data analysis, the maximum and minimum X coordinate values (Xmax, Xmin) for the static trajectory at 30 rpm were 569.2 mm and 417.5 mm, respectively. Similarly, the maximum and minimum Y coordinate values (Ymax, Ymin) were -3.1 mm and -333.3 mm, respectively. These results were very close to the trajectory obtained from simulation software. Furthermore, the result showed that the trajectory's maximum height (Ymax - Ymin) was 336.4 mm, and the maximum width (Xmax - Xmin) was 151.7 mm.

Figure 7a depicts the overlapping static trajectories generated from each method. The trajectory generated from the high-speed camera was compared with the trajectory generated from the linkage, and the result showed a deviation of 6.3 mm and 2.8 mm in terms of

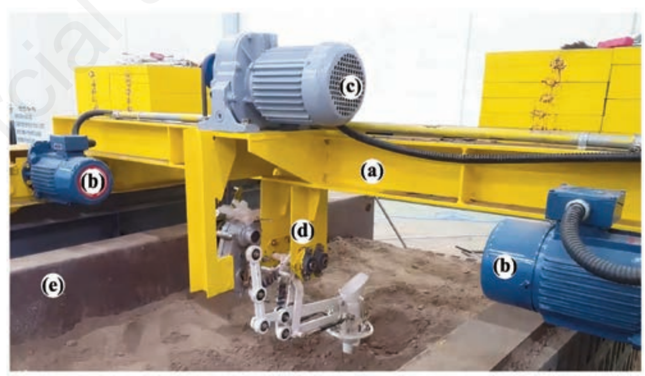

Figure 6. Set-up to test the planter unit in the soil test bin under different operating conditions. The set-up consists of: **a**) carriage; **b**) driving motors; **c**) crank motor; **d**) planter unit; **e**) soil test bin supporting structure.

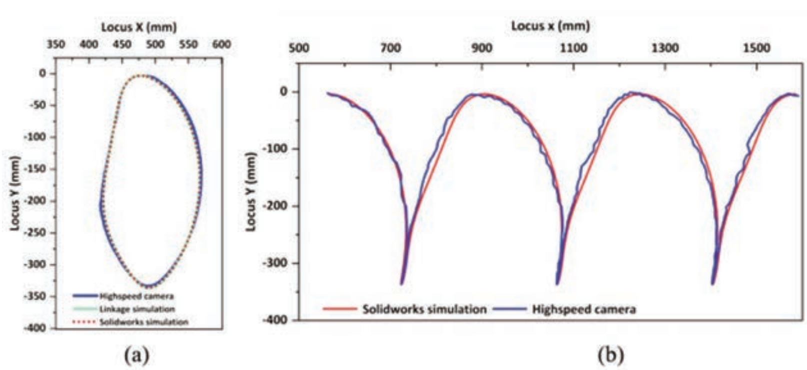

Figure 7. Graphical comparison of the simulated and extracted trajectory for (**a**) static and (**b**) dynamic conditions.

maximum width and height, respectively. Similarly, when comparing the trajectories generated from the high-speed camera and Solidworks, similar deviations by 6.3 mm and 2.8 mm in terms of maximum width and height, respectively, were obtained. The result of variance analysis for static trajectories suggested no statistical difference among the trajectories generated from the camera with the Linkage (p=0.84) and Solidworks (p=0.40), respectively. When comparing the dynamic trajectories generated from the high-speed camera and Solidworks, a deviation of 6.3 mm in maximum height was obtained. Figure 7b depicts the overlapped dynamic trajectories generated from each method. The result of ANOVA suggested no statistical difference among the dynamic trajectories generated from the camera and Solidworks (p=0.85). The minor deviation in observation may have occurred due to machine vibration during its operation. Hwang *et al*. (2020) also used the ANOVA test to compare the trajectories generated from the high-speed camera and simulation software, and found the P-value >0.05, and concluded that the simulated and actual trajectories were not statistically different. Therefore, this result concluded that the parameters used for the simulation were valid and agreed with the real conditions. Furthermore, this result suggested that any simulation condition changes would result in the same when applied to the machine's operation.

Simulation at different running speed and crank rotation

After verifying the static and dynamic trajectories, the planter mechanism was simulated for various operating conditions using Solidworks 2022 software. The operating speed was set between 150 mm/s and 350 mm/s based on the recommended ergonomic walking speed for transplanter operators suggested by the literature (Ji *et al*., 2020; Jin *et al*., 2020; Xue *et al*., 2020). For each speed, the crank rotation was simulated between 30 rpm and 80 rpm. The end of the hopper's trajectories was traced and the plant spacing (mm), soil load area (mm^2), soil intrusion perimeter (mm), and horizontal hopper displacement (mm) within the soil were calculated, assuming a theoretical planting depth of 80 mm. The results of the plant spacing from the simulation are shown in Figure 8a. The results indicate that a plant spacing of 300 mm (indicated by a red dotted line in Figure 8a) was the most optimal for this mechanism, as it was obtained for all of the simulated working speeds. The results for plant spacing, forward speed, and crank rotation satisfied the relationship described in Equation 8 (Iqbal *et al*., 2021b; Srivastava *et al*., 2006) for a single row number.

$$\text{Crank rotation} = \frac{60 \times \text{working speed} \times \text{number of rows}}{\text{Plant spacing}} \tag{8}$$

The results for the soil intrusion area (mm^2), soil intrusion perimeter (mm), and horizontal hopper displacement in soil (mm) are shown in Figure 8b-d, respectively. Equation 8 shows the relationship between crank rotation speed, working speed, and plant spacing. The crank rotation of the machine can be adjusted to

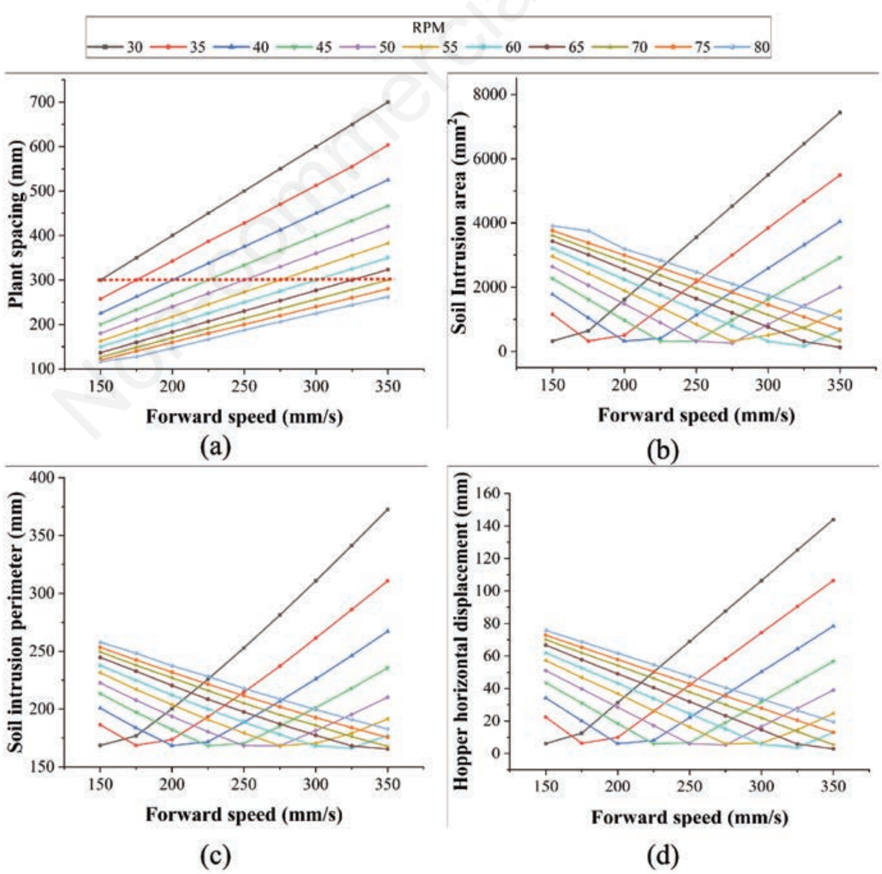

Figure 8. a) Characteristics curve obtained for plant spacing; **b**) soil intrusion area; **c**) soil intrusion perimeter; **d**) hopper horizontal displacement for the planter unit when simulated at working speed of 150 mm/s to 350 mm/s and crank rotational speed of 30 rpm to 80 rpm.

achieve the desired plant spacing at a specific working speed. However, the trajectories generated at different crank rotations should also be studied. The rate at which seedlings are supplied to the planter unit depends on the crank rotational speed and the number of rows being transplanted at a time (Srivastava *et al*., 2006).

Optimum working speed and crank rotation

The optimal working speed (mm/s) and crank rotation speed (rpm) configurations for the transplanter were chosen based on the varying planting intervals that help achieve the ideal trajectory of the transplanter. For the optimized trajectory, the planter's rotational speed should be synchronized with the machine's forward speed and other mechanisms, such as seedling pickup and metering (Islam *et al*., 2020). This study selected working speeds of 200 mm/s, 250 mm/s, and 300 mm/s, which had a speed difference of 50 mm/s between each gear shift. These speeds were chosen based on the comfortable walking range of 150 to 350 mm/s, considering the ergonomics for the operator to walk behind the machine (Ji *et al*., 2020; Jin *et al*., 2020; Xue *et al*., 2020). Some literature suggests that the transplanting performance is affected by the working speed of the machine, with extremely low and very high speeds resulting in improper transplantation with shallow planting depth and large planting angle (Iqbal *et al.*, 2021b). To avoid this variation, speeds within the range, close to the mean values, were selected. The speed difference of 50 mm/s was chosen based on the speed difference found on commercial transplanters during each gear shift.

To select the appropriate crank speed for each working speed, the simulated results with the minimum soil intrusion area, intrusion perimeter, and horizontal displacement of the hopper in soil were considered. For a working speed of 200 mm/s, the minimum soil intrusion area (324.1 mm^2), intrusion perimeter (168.4 mm), and horizontal hopper displacement in soil (6.0 mm) were obtained at a crank rotation of 40 rpm. Similarly, for a working speed of 250 mm/s, the minimum soil intrusion area (319.6 mm^2), intrusion perimeter (168.3 mm), and horizontal hopper displacement in soil (6.00 mm) were obtained at a crank rotation of 50 rpm. At a working speed of 300 mm/s, the minimum values for soil intrusion area, intrusion perimeter, and horizontal hopper displacement were found to be 314.4 mm^2, 168.1 mm, and 5.7 mm, respectively, at a crank rotation of 60 rpm. In summary, working speeds of 200, 250, and 300 mm/s were selected as the machine's forward speed with crank rotations of 40, 50, and 60 rpm as a new combination for the existing transplanter. The trajectories generated from each speed and crank rotation combination are shown in Figure 9. Along with the machine operating speed configurations, the X component of horizontal velocity in the forward direction (v_x) of the hopper end was simulated and the results are presented in Table 1. The results suggest that the configuration that results in the minimum intrusion area, perimeter, and horizontal hopper displacement in soil also results in the minimum horizontal velocity of the hopper at the lowest position inside the soil.

Testing of the planter mechanism

The selected combination of working speed and crank rotation was tested with the planter unit at the soil test bin facilities at Gyeongsang National University. The soil in the test bin was analyzed for texture using sedimentation tests and found to be of sandy loam type, with an average composition of 84.8% sand, 9.8% silt, and 5.4% clay. The sampled soil had an EC of 24.40 mS/cm, pH of 6.53, soil temperature of 17.17°C at the time of test-

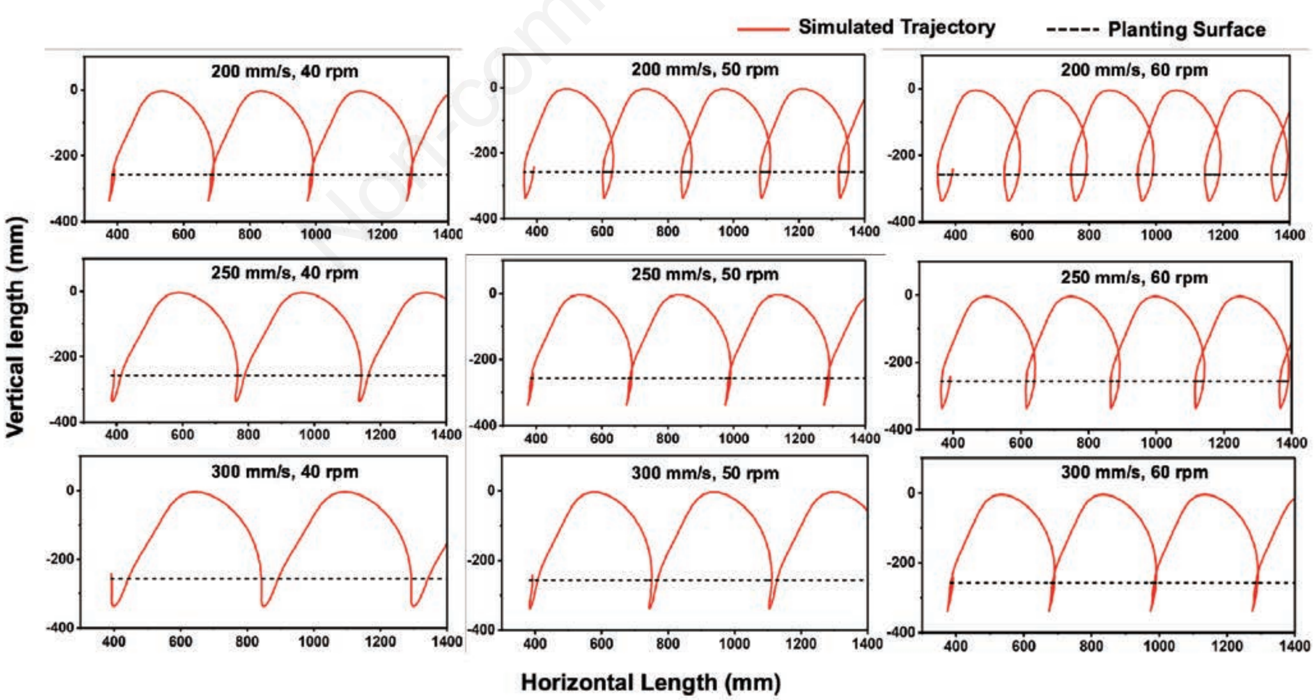

Figure 9. The simulated trajectories of the linkage-type planting unit at 200, 250, and 300 mm/s and rpm of 40, 50, and 60. The selected speeds and rpm were chosen to test with a planter unit in soil bin.

ing, wet bulk density of 1.42 g/cm^3, dry bulk density of 1.23 g/cm^3, and moisture content of 13.36% (dry basis). To test the planting performance of the planter unit, 45-day-old pepper seedlings grown in biodegradable seedling plug trays were used. The properties of 20 randomly selected pepper seedlings were tested, and the average plant height, leaf area, fresh weight, and dry weight were found to be 221.3 mm, 15.09 cm^2, 2.99 g, and 0.40 g, respectively. The average weight of an individual seedling, including the biodegradable plug cell and potting media (bioplus compost) with an average moisture content of 62% (dry basis), was 22.72 g. The average size of the plug cell was 30×30 mm at the top, 20×20 mm at the base, and 42 mm in height. During testing, each plug cell with a seedling was manually fed into the hopper when it was in its topmost position.

The results from the test bin experiment (Table 2) showed that the plant spacings obtained during the experiment were very close to the results obtained from the simulated conditions. At a forwarding speed of 200 mm/s and crank rotations of 40, 50, and 60 rpm, the average plant spacing was found to be 298±9 mm, 240±7 mm, and 199±8 mm, respectively, which were very similar to the simulated results of 300 mm, 240 mm, and 200 mm, respectively. At a forwarding speed of 250 mm/s and crank rotations of 40, 50, and 60 rpm, the average planting distance was found to be 375±5 mm, 299±10 mm, and 245±11 mm, respectively, which were also similar to the simulated results of 375 mm, 300 mm, and 250 mm, respectively. Similarly, at a forwarding speed of 300 mm/s and crank rotations of 40, 50, and 60 rpm, the experimented plant spacings were found to be 453±13 mm, 365±18 mm, and 305±18 mm, respectively, very close to the simulated results of 450 mm, 360 mm, and 300 mm, respectively. On analyzing the overall data obtained, a maximum variation of up to 8.5% was found between theoretical and actual measurements, with an average variation of 3%. This suggests that the actual measurement values were very close to the theoretical measurements. The statistical analysis showed no significant difference in actual planting intervals between 200 mm/s and 40 rpm, 250 mm/s and 50 rpm, and 300 mm/s and 60 rpm, whose theoretical plant spacing was 300 mm. Additionally, the combination of 200 mm/s and 50 rpm, and 250 mm/s and 60 rpm speeds also had no statistical difference in actual planting intervals. Overall, the nine different speed combinations resulted in five statistically significant planting intervals ranging from 200 mm to 450 mm.

The average planting depths during the test bin experiment were found to be 81±8 mm, 82±4 mm, and 77±8 mm, at 40, 50, and 60 rpm of crank rotation, respectively, at a working speed of 200 mm/s. For the same configuration, the planting angles were 4.2±1.2°, 6.8±1.5°, and 9.0±2.3°, respectively. Similarly, planting depths of 78±11 mm, 80±13 mm, and 79±13 mm were found at 40, 50, and 60 rpm of crank rotations, respectively, with corresponding planting angles of 8.3±1.8°, 6.6±1.2°, and 9.4±2.1°, respectively, at a forwarding speed of 250 mm/s. Finally, at a forwarding speed of 300 mm/s and 40, 50, and 60 rpm of crank rotations, the planting depths were 75±15 mm, 74±13 mm, and 72±18 mm, respectively, with corresponding planting angles of 9.3±2.4°, 10.7±3.1°, and 8.6±2.1°, respectively. On comparing actual and theoretical planting depths, a maximum variation of 43% was obtained at

Table 1. The X component of the linear velocity of the hopper endpoint toward the forward direction. The table represents data with X component (forward direction) maximum velocity, minimum velocity, and the velocity at the lowest position of the hopper (representing the seedling deposition position).

Speed (mm/s)	Crank rotation (rpm)	Maximum velocity (mm/s)	Minimum velocity (mm/s)	Hopper lowest position velocity (mm/s)
200	40	596.19	-110.96	3.28
	50	695.68	-184.88	-29.43
	60	794.29	-266.44	-54.77
250	40	646.19	-60.96	28.03
	50	745.68	-134.88	-4.14
	60	844.29	-216.44	-20.21
300	40	696.19	-10.96	48.00
	50	795.68	-84.88	14.67
	60	894.29	-166.44	-12.17

Table 2. Summary of the result (mean ± standard deviation) obtained from the soil test bin experiment of the planter unit at 200, 250, and 300 mm/s of running speed and 40, 50, and 60 rpm of crank rotation speed.

Speed (mm/s)	Crank rotation (rpm)	Plant spacing (mm)	Planting depth (mm)	Planting angle (°)	Mulch damage (mm^2)
200	40	298±9^{c}	81±8^{a}	4.2±1.0^{a}	3479±233^{a}
	50	240±7^{b}	82±4^{a}	6.8±1.5^{ab}	4583±138^{c}
	60	199±8^{a}	77±8^{a}	9.0±2.3^{bc}	5456±250^{d}
250	40	375±5^{d}	78±11^{a}	8.3±1.8^{bc}	4361±320^{c}
	50	299±10^{c}	80±13^{a}	6.6±1.2^{ab}	3519±375^{a}
	60	245±11^{b}	79±13^{a}	9.4±2.1^{bc}	4452±396^{c}
300	40	453±13^{e}	75±15^{a}	9.3±2.4^{bc}	5863±430^{d}
	50	365±18^{d}	75±13^{a}	10.7±3.1^{c}	4179±374^{bc}
	60	305±13^{c}	72±18^{a}	8.6±2.1^{bc}	3705±516^{ab}

Different letters in the same column denote significant differences in the measured values at $p \leq 0.05$ based on Tukey's honestly significant difference post-hoc test.

higher speed configurations; however, the average variation was found to be 17%. Despite the large variation, the planting depths obtained from all the speed configurations were statistically similar (P=0.75). In contrast, the planting angles obtained from different speed combinations were significantly different.

Regarding mulch film damage, the field test recorded the lowest damage of 3479±233 mm^2 at the 200 mm/s and 40 rpm speed combinations, while the highest damage (5863±430 mm^2) occurred at the 300 mm/s and 40 rpm speed combination. According to statistical analysis, the optimized trajectory that resulted in a plant spacing of 300 mm (200 mm/s and 40 rpm; 250 mm/s and 50 rpm; 300 mm/s and 60 rpm) showed no significant difference in terms of mulch film damage caused by the hopper. A strong correlation (r=0.91) was found between the hopper's horizontal displacement calculated from the simulation test and the actual mulch film damage, indicating that the selected working speeds with the minimum hopper horizontal displacement were a suitable choice, causing less damage to the mulch film compared to other simulated speed combinations.

The results from the field testing of the chosen speed configurations depicted that, as the forward speed increases, the variations in planting depths and planting angles also increase, which is similar to the findings of Iqbal *et al*. (2021), but the obtained planting angles were within the permissible limits (±20°). Furthermore, the most optimized planter trajectory had a plant spacing of 300 mm, which was obtained at all the working speeds tested with different crank rotation combinations. The nine different speed combinations tested had different plant spacings ranging from 200 mm to 450 mm, which were within the agronomic plant spacing for most vegetable crops (Maynard and Hochmuth, 2007).

Conclusions

In this study, the ability of a linkage-type planter mechanism for an automated biodegradable seedling-plug vegetable transplanter to operate at different running speeds and crank rotation combinations was analyzed. To do this, the mechanism of the planter units was studied and designed using simulation software such as Linkage and SolidWorks to draw its working trajectories and verify them with the actual trajectory of the planter unit, which was generated using a high-speed camera. After verifying the existing trajectory, the planter unit was simulated at different running and rotation speed combinations, generating the working trajectory in each combination. The trajectories that tended to meet the requirements of ideal conditions were selected and tested with a planter unit in soil test bin conditions. The simulation results verified the optimum planting spacing of 300 mm, which was achieved in each working speed combination ranging from 150 mm/s to 300 mm/s. Taking references from the design of other vegetable transplanters, working speeds of 200, 250, and 300 mm/s were selected with planter rotational speeds of 40, 50, and 60 rpm, which tended to satisfy the ideal trajectory conditions. Testing the planter unit in test bin conditions revealed that the tested working and rotational speed combinations showed good feasibility when transplanting pepper seedlings. The plant spacing during testing was very similar to that of the simulated condition, and the planting angle (seedling uprightness) and planting depth in each case were within permissible limits. Testing the planter in controlled conditions, *i.e.*, soil test bins, may result in low variation of the planting depth and planting angle compared to field test results as in other literature. However, the variation may increase if the machine is tested in the field with necessary modifications, as several factors such as air drag, traction, soil strength, wheel slip, and skid can affect the machine's performance. In this study, the automated transplanter was tested at working speeds of 200, 250, and 300 mm/s, and the other mechanisms will be optimized based on the optimal speed determined for the transplanter. The results of this study could potentially be useful for speeding up the process of mechanizing automated seedling transplanting operations.

References

Dou, Z., Li, Y., Guo, H., Chen, L., Jiang, J., Zhou, Y., Xu, Q., Xing, Z., Gao, H., Zhang, H. 2021. Effects of mechanically transplanting methods and planting densities on yield and quality of nanjing 2728 under rice-crayfish continuous production system. Agronomy 11:488.

Du, S., Yu, J., Wang, W. 2018. Determining the minimal mulch film damage caused by the up-film transplanter. Adv. Mech. Eng. 10:168781401876677.

Durga, M.L., Rao, A.S., Kumar, A.A. 2020. Performance evaluation of single row-low horse power tractor operated vegetable transplanter. Curr. J. Appl. Sci. Technol. 37-44.

Edmonds, W.A., Kennedy, T.D. 2017. An applied guide to research designs: quantitative, qualitative, and mixed methods. SAGE Publications, Thousand Oaks, California.

Hwang, S.-J., Park, J.-H., Lee, J.-Y., Shim, S.-B., Nam, J.-S. 2020. Optimization of main link lengths of transplanting device of semi-automatic vegetable transplanter. Agronomy 10:1938.

Iqbal, M.Z., Islam, M.N., Ali, M., Kabir, M.S.N., Park, T., Kang, T.-G., Park, K.-S., Chung, S.-O. 2021a. Kinematic analysis of a hopper-type dibbling mechanism for a 2.6 kW two-row pepper transplanter. J. Mech. Sci. Technol. 35:2605-14.

Iqbal, M.Z., Islam, M.N., Chowdhury, M., Islam, S., Park, T., Kim, Y.-J., Chung, S.-O. 2021b. Working speed analysis of the gear-driven dibbling mechanism of a 2.6 kW walking-type automatic pepper transplanter. Machines 9:6.

Islam, M.N., Iqbal, M.Z., Ali, M., Chowdhury, M., Kabir, M.S.N., Park, T., Kim, Y.-J., Chung, S.-O. 2020. Kinematic analysis of a clamp-type picking device for an automatic pepper transplanter. Agriculture 10:627.

Islam, M.N., Iqbal, M.Z., Ali, M., Chowdhury, M., Kiraga, S., Nur Kabir, M.S., Lee, D.-H., Woo, J.-K., Chung, S.-O. 2022. Theoretical transmission analysis to optimize Gearbox for a 2.6 kW automatic pepper transplanter. J. Agric. Eng.

Ji, J., Cheng, Q., Jin, X., Zhang, Z., Xie, X., Li, M. 2020. Design and test of 2ZLX-2 transplanting machine for oil peony. Int. J. Agric. Biol. Eng. 13:61-9.

Jin, X., Cheng, Q., Zhao, B., Ji, J., Li, M. 2020. Design and test of 2ZYM-2 potted vegetable seedlings transplanting machine. Int. J. Agric. Biol. Eng. 13:101-10.

Jo, J.S., Okyere, F.G., Jo, J.M., Kim, H.T. 2018. A study on improving the performance of the planting device of a vegetable transplanter. J. Biosyst. Eng. 43:202-10.

Kalmpourtzidou, A., Eilander, A., Talsma, E.F. 2020. Global vegetable intake and supply compared to recommendations: a systematic review. Nutrients 12:1558.

Kumar, G.V.P., Raheman, H. 2008. Vegetable transplanters for use in developing countries—a review. Int. J. Veg. Sci. 14:232-55.

Kumar, G.V.P., Raheman, H. 2011. Development of a walk-behind type hand tractor powered vegetable transplanter for paper pot seedlings. Biosyst. Eng. 110:189-97.

Liu, T., Hou, S., Zhao, X., Yin, L., Yin, C., Wang, Q. 2009. Computer aided analysis of planting mechanism of the seedling transplanter. 2009 International Conference on Measuring Technology and Mechatronics Automation. IEEE. pp. 38-41.

Maynard, D.N., Hochmuth, G.J. 2007. Knott's handbook for vegetable growers, 5th ed. John Wiley and Sons Inc, Hoboken, New Jersey.

Park, J.-H., Hwang, S.-J., Nam, J.-S. 2018. Operational characteristics of a domestic commercial semi-automatic vegetable transplanter. J. Agric. Life Sci. 52:127-38.

Park, S.H., Cho, S.C., Kim, J.Y., Choi, D.K., Kim, C.K., Kwak, T.Y. 2005a. Development of rotary type transplanting device for vegetable transplanter. J. Biosyst. Eng. 30:135-40.

Park, S.H., Kim, J.Y., Choi, D.K., Kim, C.K., Kwak, T.Y., Cho, S.C. 2005b. Development of walking type chinese cabbage transplanter. J. Biosyst. Eng. 30:81-8.

Paudel, B., Basak, J.K., Kaushalya Madhavi, B.G., Kim, N.-E., Lee, G.-H., Choi, G.-M., Choi, Y.-W., Kim, H.T. 2022. Properties of paper-based biodegradable pots for growing seedlings. Hortic. Environ. Biotechnol. 63:793-807.

Reza, M.N., Islam, M.N., Chowdhury, M., Ali, M., Islam, S., Kiraga, S., Lim, S.-J., Choi, I.-S., Chung, S.-O. 2021. Kinematic analysis of a gear-driven rotary planting mechanism for a six-row self-propelled onion transplanter. Machines 9:183.

Shim, S., Kim, Y., Yang, S., Lee, S., Lee, D. 2016. A study on trace of hopper of the transplanter. Korean Soc. Agric. Mach. pp. 201–202.

Sri, M., Hwang, S.-J., Nam, J.-S. 2022. Experimental safety analysis of transplanting device of the cam-type semi-automatic vegetable transplanter. J. Terramech. 103:19-32.

Srivastava, A.K., Goering, C.E., Rohrbach, R.P., Buckmaster, D.R. 2006. Engineering principles of agricultural machines, 2nd ed. Am. Soc. Agric. Biol. Eng.

Statistics Korea. 2021. Agriculture, Forestry and Fishery Survey in 2021. Available from: http://kostat.go.kr/. URL http://kostat.go.kr/portal/eng/index.action (accessed on 22nd December, 2022).

Tsuga, K. 2000. Development of fully automatic vegetable transplanter. Japan Agric. Res. Q. 34:21-28.

Wen, Y., Zhang, J., Tian, J., Duan, D., Zhang, Y., Tan, Y., Yuan, T., Li, X. 2021. Design of a traction double-row fully automatic transplanter for vegetable plug seedlings. Comput. Electron. Agric. 182:106017.

Xue, X., Li, L., Xu, C., Li, E., Wang, Y. 2020. Optimized design and experiment of a fully automated potted cotton seedling transplanting mechanism. Int. J. Agric. Biol. Eng. 13:111-17.